Earth and Planetary Science
https://journals.nasspublishing.com/index.php/eps

ARTICLE

Shock-Related Microstructural Deformation in Zircon from the Colônia Impact Crater, Brazil

Victor Velázquez Fernandez [1*] ***, José Maria Azevedo Sobrinho*** [2] ***, Rodrigo Ferreira Lucena*** [1] ***, Alethéa Ernandes Martins Sallun*** [2] ***, William Sallun Filho*** [2]

[1] *School of Arts, Sciences, and Humanities, University of São Paulo, São Paulo CEP 03828-000, Brazil*

[2] *Environmental Research Institute, Secretariat for the Environment, Infrastructure and Logistics, São Paulo CEP 04015-011, Brazil*

ABSTRACT

Microdeformation features in zircon grains from borehole samples of the Colônia impact crater were characterized by transmitted-light petrography. High-resolution polarized-light images of 40 zircon grains (>50 μm), selected from 200 polished thin sections, were used to determine crystallographic orientations, classify textural domains, and characterize stress-induced microstrain features. Zircon morphologies comprise 67% euhedral, 30% subhedral or fragmented, and 3% anhedral or rounded crystals, with sizes ranging from 30 to 150 μm. Euhedral prismatic crystals, elongated parallel to the c-axis, display aspect ratios of 3:1–4:1; rounded grains yield lower ratios approaching 2:1. Microstructural analysis of six representative grains—three euhedral and three subhedral—reveals five distinct deformation types: (i) recrystallization, (ii) crystallographic misorientation, (iii) growth-zone disorder, (iv) planar deformation features (PDFs), and (v) granular textures. Euhedral grains with metamorphic relict cores predominantly exhibit recrystallization and crystallographic misorientation, consistent with intense thermomechanical overprinting. Subhedral crystals of igneous origin, by contrast, are dominated by granular textures and PDFs, recording dynamic recrystallization and shock metamorphism under high-strain conditions. The presence of PDFs unequivocally establishes a shock origin; the remaining microstructures record progressive deformation

*CORRESPONDING AUTHOR:
Victor Velázquez Fernandez, School of Arts, Sciences, and Humanities, University of São Paulo, São Paulo CEP 03828-000, Brazil; E-mail: vvf@usp.br

ARTICLE INFO
Received: 31 January 2026 | Revised: 13 March 2026 | Accepted: 18 March 2026 | Published Online: 26 March 2026
DOI: https://doi.org/10.36956/eps.v5i1.3117

CITATION
Fernandez, V.V., Sobrinho, J.M.A., Lucena, R.F., et al., 2026. Shock-Related Microstructural Deformation in Zircon from the Colônia Impact Crater, Brazil. Earth and Planetary Science. 5(1): 47–61. DOI: https://doi.org/10.36956/eps.v5i1.3117

across a range of pressure–temperature conditions. These microdeformation patterns reflect anisotropic strain imposed by impact-generated shock waves, which preferentially affected the mechanically weaker prismatic faces {100} and {110}. Taken together, the results confirm the reliability of zircon as a recorder of extreme tectonothermal events and provide crystallographic constraints for post-impact structural reconstructions.
Keywords: Colônia Impact Crater; Zircon Crystal; Microdeformation Features; Shock Metamorphism

1. Introduction

Zircon ($ZrSiO_4$) occupies a central role in shock metamorphism studies, providing critical insights into the processes involved in impact crater formation across diverse geological settings [1]. Owing to its exceptional resistance to thermal and chemical alteration during metamorphism and weathering, zircon ranks among the most stable minerals in the Earth's crust and preserves both microstructural and geochemical evidence of high-energy events [2]. These properties establish zircon as an effective mineralogical archive of extreme conditions, distinguishing it from other rock-forming minerals [3].

Impact cratering generates abrupt, extreme increases in pressure and temperature, inducing profound mineralogical transformations in target rocks [4,5]. In zircon, such conditions produce diagnostic structural modifications, most notably the formation of reidite—a high-pressure polymorph that crystallizes at pressures exceeding ~30 GPa [6,7]. Reidite is widely regarded as a robust, unambiguous indicator of shock metamorphism associated with impact events [8,9]. Zircon may also preserve a range of other shock-related microstructures, including PDFs and mechanical twins, which typically develop under intermediate shock pressures [10]. A further distinctive microstructural signature is the granular FRIGN (fragmented reidite-inherited granular neoblastic) texture, interpreted as the product of zircon recrystallization during post-shock cooling [11]. This texture results either from reidite breakdown or from thermally driven recrystallization associated with the dissipation of impact-generated heat [12,13].

The significance of zircon extends beyond the preservation of shock-related microstructures to encompass geochronological applications, particularly U–Pb dating, owing to its exceptional capacity to retain radiogenic isotopes over billion-year timescales [14]. Impact events can partially disrupt this isotopic system, inducing lead loss or elemental redistribution within zircon crystals. Consequently, shocked zircon provides a powerful means of directly dating impact events and constraining the timing of major impacts that have shaped Earth's geological evolution [15–17].

Studies of the Chicxulub impact structure in Mexico exemplify the application of zircon in impact research [17,18]. This crater is associated with the Cretaceous–Paleogene mass extinction event at ~66 Ma, and zircon grains recovered from its peak ring preserve clear evidence of shock metamorphism, including reidite and granular FRIGN textures. These microstructural indicators have enabled reconstruction of the pressure–temperature conditions generated during the impact, providing key constraints on the scale and intensity of this globally significant event.

Shocked zircon has also been employed as a diagnostic indicator in other impact structures, such as the Mien crater in Sweden [19]. In these settings, the identification of shock-related microstructures combined with zircon geochronology has significantly improved the calibration of shock barometers and refined models for the formation of complex impact craters.

The Colônia impact crater represents an atypical example among deeply eroded impact structures, owing to its distinctive geological setting and remarkable degree of preservation. Unlike many comparably degraded structures—where primary textures and shock-metamorphic indicators are largely obliterated by intense weathering—Colônia retains a broad spectrum of shock-related microstructures in zircon and associated mineral phases, principally quartz, feldspar, and mica [20]. Despite this preservation potential, the structure remains comparatively underexplored. Here, high-resolution petrography is integrated with systematic zircon microstructural analysis to provide a compre-

hensive characterization of shock-metamorphic features within the crater. The documented preservation patterns impose new constraints on the stability and long-term survivability of deformation microstructures under prolonged weathering conditions. Furthermore, these results establish a comparative framework for evaluating other deeply eroded or strongly altered impact structures.

2. Geological Framework

The Colônia Crater, located in the Parelheiros district, approximately 40 km southwest of downtown São Paulo (**Figure 1a,b**), has a diameter of ~3.6 km and forms a well-defined circular structure of geological and geomorphological significance. Since its initial documentation, this distinctive depression has attracted sustained scientific interest owing to its morphology, which is consistent with structures formed by the impact of extraterrestrial bodies[21]. The crater is situated within the Ribeira Belt, a major Neoproterozoic orogenic province of southeastern Brazil. The regional crystalline basement consists of metamorphic and igneous lithologies of the Embu Complex, including mica schists, quartzites, gneisses, migmatites, granites, and granodiorites (**Figure 1c**), into which the crater is emplaced[22]. Geophysical surveys reveal that, below the crater, these basement rocks occur at 285–400 m[23–25]. Subsequent investigations[26–30] have been critical for characterizing the sedimentary infill of the Colônia crater. Seismic data indicate that the sedimentary succession reaches thicknesses of up to ~275 m[30]. Samples recovered from groundwater-extraction boreholes penetrating depths greater than 280 m reveal a heterogeneous assemblage of impactite lithologies, which is largely composed of allochthonous polymictic breccia, suevite breccia, and fractured/brecciated crystalline basement rocks[20,31] (**Figure 1d**).

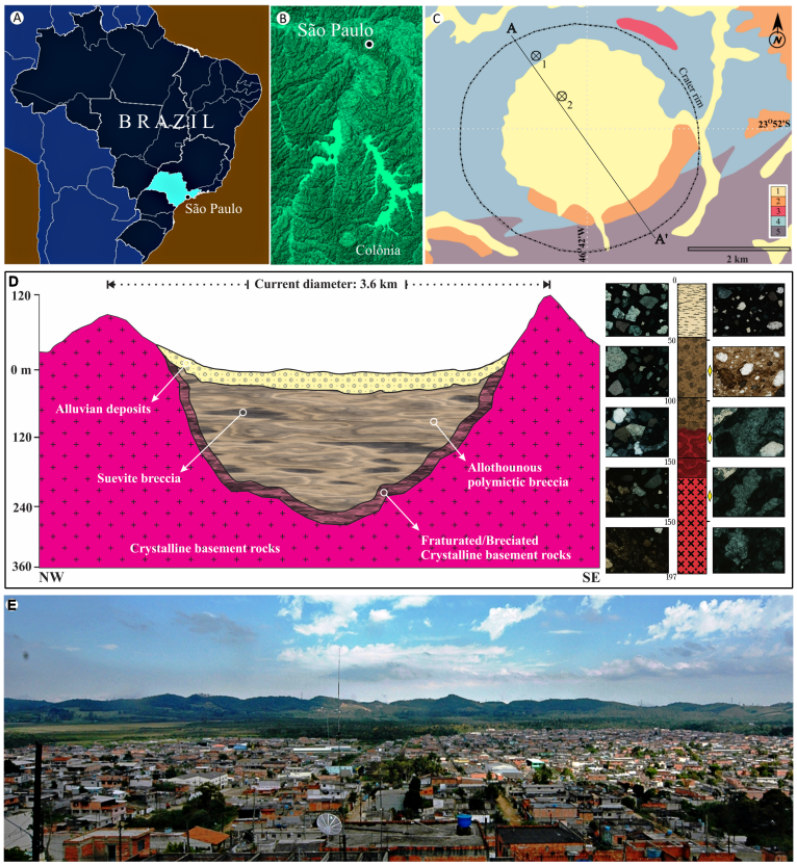

Figure 1. Location and geological context of the Colônia impact crater. (**a,b**) Regional and local maps; (**c**) Modified schematic geological map[22,28]; (**d**) Representative stratigraphic column[20]; (**e**) The Vargem Grande neighborhood is encircled by the prominent southwestern crater rim visible in the background.

Note: Legends for **Figure 1c**: (1) Quaternary alluvial deposits; (2) Tertiary sediments; (3) Diorite and quartz diorite; (4) Mica schist and quartzite; (5) Gneiss and migmatite. Drillhole locations according to Velázquez et al.[19,30,31]: ⊕1 and ⊕2. A–A' segment: stratigraphic column location.

Given its morphological characteristics, the Colônia structure constitutes the dominant topographic feature of the local landscape. The interior of the crater consists of a swampy alluvial plain surrounded by low-relief hills with gentle slopes that rise to about 125 m above the crater floor [28]. Currently, it is partially covered by remnants of the Atlantic Forest, which are increasingly affected by anthropogenic activity, mainly associated with the expansion of the Vargem Grande neighborhood (**Figure 1e**).

The impact origin of the structure is conclusively demonstrated by multiple shock-metamorphism indicators, including PDFs in quartz, kink bands in mica, granular textures in zircon, and ballen silica [20]. Impact-melt rocks, including spherules formed by vaporization and rapid cooling of target material, provide unequivocal evidence for an impact-cratering origin [31–33].

3. Materials and Methods

High-resolution digital images were obtained from zircon crystals >50 μm in size using 200 standard petrographic thin sections (30 μm thickness) prepared by Activation Laboratories Ltd. (Ancaster, Canada). The samples derive from boreholes located within the crater interior (**Figure 1c**) and were previously investigated by Velázquez et al. [19,30,31]. To ensure analytical robustness, only inclusion-free and fracture-free grains lacking optical interference were selected for analysis. Each zircon was systematically examined under polarized light to assess textural preservation and to assign it to the principal genetic categories, distinguishing magmatic from metamorphic-recrystallized domains. This screening protocol enabled the consistent identification of the dominant zircon populations within the analyzed lithologies.

Crystallographic orientations of the selected grains were subsequently determined using an Olympus BX51 petrographic microscope, integrating grain morphology, optical properties, and theoretical crystallographic models [34–36]. From the total population of zircons examined, 40 grains were selected for detailed analysis. This subset was chosen to ensure representative coverage of the main lithological units and sampled depth intervals, while balancing statistical robustness with the practical constraints inherent to grain-scale analytical methods.

Optical images were acquired under cross-polarized light at 10° rotation increments to enhance the identification and discrimination of microdeformation features. Deformation microstructures were classified according to their morphology and optical properties, including geometry, crystallographic orientation, cross-cutting relationships, and birefringence behavior. The identified features comprise: (i) undulatory extinction bands, interpreted as indicative of crystal-plastic deformation and/or recrystallization; (ii) closely spaced, planar microfractures consistent with PDFs; (iii) sharp extinction boundaries associated with granular textures; and (iv) isotropic to weakly birefringent domains interpreted as evidence of metamictization.

The software ImageJ, MTEX for MATLAB, and Gwyddion were utilized for image processing and quantitative analysis. Adaptive threshold segmentation [37] was applied to isolate internal deformation features and quantify their structural orientations. The relative degree of deformation in each grain was calculated from the segmented deformation domains and expressed as the ratio between their cumulative area and the total grain area, providing a quantitative basis for comparing deformation intensity among individual zircon grains.

4. Morphology, Primary Structures, and Microdeformations

The external morphology of the 40 analyzed zircon crystals exhibits considerable variation. Of these, 67% are euhedral, 30% are subhedral or fragmented, and 3% are anhedral or display rounded edges (**Figure 2a**). Most grains are relatively small, with sizes ranging from 30 to 150 μm. Crystals with prismatic faces oriented parallel to the c-axis display aspect ratios of 3:1 to 4:1, whereas more equidimensional grains yield ratios closer to 2:1. Under plane-polarized light, the crystals are predominantly colorless, indicating a good state of preservation; however, some grains locally exhibit a faint brownish hue, potentially attributable to compositional heterogeneity, microscopic inclusions, or incipient metamictization. Most grains exhibit well-developed oscillatory

growth zoning; its absence, restricted to a limited number of crystals, likely reflects recrystallization, chemical homogenization, or post-crystallization modification. Based on these internal structural characteristics [38], two principal zircon groups are distinguished: grains with irregular zoning—commonly displaying inherited cores and heterogeneous internal structures—are interpreted as metamorphic in origin, whereas grains with concentric, symmetrical zoning are interpreted as magmatic. Although primary growth zoning is preserved in most crystals, it is locally modified or partially obliterated in association with shock-metamorphic microstructural features, including recrystallization textures, crystallographic misorientation, disrupted growth zoning, planar deformation features (PDFs), and granular textures (**Figure 2b**).

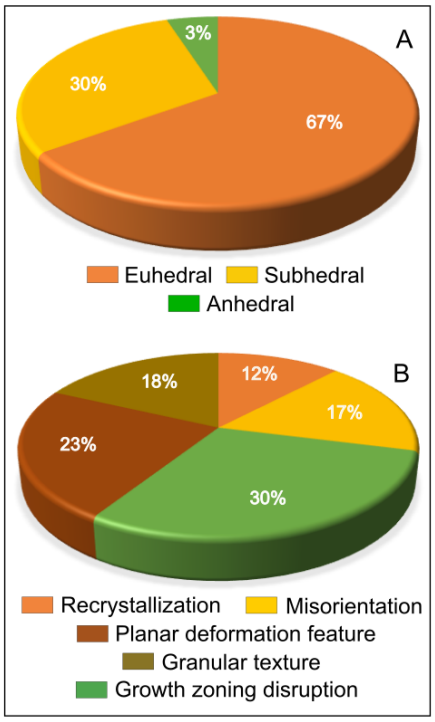

Figure 2. Graphs illustrating the morphological and microstructural characteristics of the 40 analyzed crystals. (**a**) Relative proportions of crystal morphologies; (**b**) Relative abundances of the main microdeformation features.
Note: Detailed descriptions and morphological characteristics of the zircon types are provided in Section 5.

5. Shock-Induced Metamorphic Features

Of the 40 analyzed grains, six representative zircons were selected for detailed microstructural investigation: three euhedral crystals containing metamorphic relict cores (Grains 1–3) and three subhedral grains of magmatic origin (Grains 4–6). All selected grains are exceptionally well preserved, displaying sharply defined crystal faces and well-developed primary growth zoning. This preservation state permits a robust characterization of shock-metamorphic features.

5.1. Grain 1

The euhedral zircon crystal exhibits an aspect ratio of approximately 2:1, defined by well-developed prismatic faces {100} and subdued pyramidal terminations {101}. Its longest dimension in the image face is oriented parallel to the crystallographic c-axis (**Figure 3**, Grain 1). Growth zoning is pervasively disrupted, manifesting as curved, distorted, and locally discontinuous patterns with distinct lateral offsets, rather than well-defined concentric arrangements (**Figure 3**, Grain 1A). In several domains, interference colors are locally attenuated or partially suppressed. Recrystallization is evidenced by diffuse internal boundaries, gradual variations in interference colors, and pervasive undulatory extinction throughout the crystal (**Figure 3**, Grain 1B). The occurrence of subgrains with discrete extinction angles and distinct crystallographic misorientations further corroborates intracrystalline reorganization (**Figure 3**, Grain 1C). Planar deformation features are developed within domains of pronounced birefringence variation and occur as closely spaced, parallel lamellae, locally oriented obliquely with respect to one another (**Figure 3**, Grain 1B, C). Stage rotation reveals small, irregularly bounded neoblasts within the pyramidal sector; these exhibit low birefringence and mosaic extinction, indicative of incipient granular texture development.

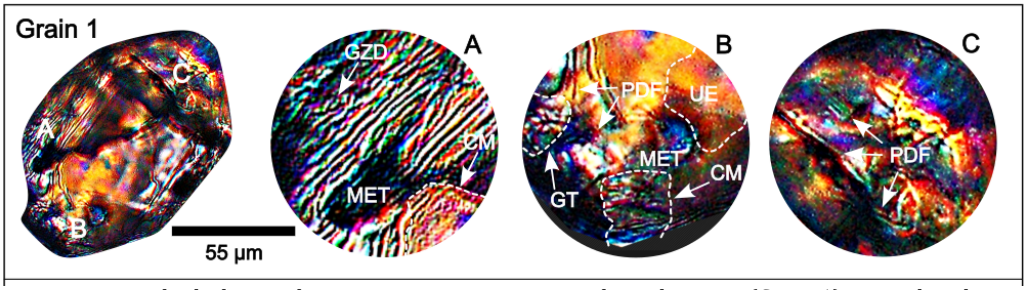

Figure 3. Representative euhedral crystal zircon containing metamorphic relict core (Grain 1) imaged under cross-polarized light, illustrating a range of internal microstructural features related to shock deformation.

Note: Left panels show full-grain views, whereas circular panels (A–C) present higher-magnification images of selected domains. The zircons record complex deformation patterns, including PDFs, granular textures (GT), disturbed growth zoning (GZD), inherited cores (IC), crystallographic misorientation (CM), metamict domains (MET), and undulatory extinction (UE). The spatial distribution and overprinting relationships among these features indicate heterogeneous shock strain accommodation at the grain scale.

5.2. Grain 2

The crystal exhibits moderate to high interference colors and an elongated morphology with an aspect ratio of approximately 4:1, terminating in slightly rounded pyramidal faces. The long axis is oriented parallel to the crystallographic c-axis, permitting clear observation of the prismatic face {110} (**Figure 4**, Grain 2). Secondary overgrowth domains are locally developed and are distinguished from the relict core by diffuse internal boundaries and undulatory extinction. Growth zoning is pervasively disrupted (**Figure 4**, Grain 2A): concentric zoning patterns are deformed, growth bands are abruptly truncated by intragranular fractures, and zoning is partially attenuated or obliterated in localized domains. The intragranular fractures display variable orientations and exhibit both dextral and sinistral apparent offsets. Planar deformation features occur as closely spaced, narrow, rectilinear lamellae oriented parallel to one another and aligned along specific crystallographic faces, including {100} and {101}. Under face-polarized light, these lamellae are difficult to resolve owing to their low relief and limited birefringence contrast; they are locally expressed as faint linear traces or as subtle birefringence variations (**Figure 4**, Grain 2B, C). The lamellae intersect and locally truncate primary growth zoning and are spatially associated with intragranular fractures. Granular textures are widespread, comprising variably sized microdomains distributed irregularly throughout the crystal. These domains locally modify birefringence intensity (**Figure 4**, Grain 2C) and produce undulatory to mosaic extinction patterns.

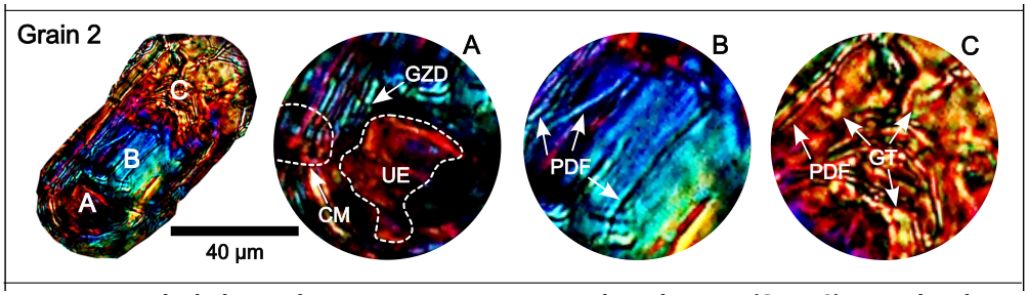

Figure 4. Representative euhedral crystal zircon containing metamorphic relict core (Grain 2) imaged under cross-polarized light, illustrating a range of internal microstructural features related to shock deformation.

Note: Left panels show full-grain views, whereas circular panels (A–C) present higher-magnification images of selected domains. The zircons record complex deformation patterns, including PDFs, granular textures (GT), disturbed growth zoning (GZD), inherited cores (IC), crystallographic misorientation (CM), metamict domains (MET), and undulatory extinction (UE). The spatial distribution and overprinting relationships among these features indicate heterogeneous shock strain accommodation at the grain scale.

5.3. Grain 3

The zircon crystal exhibits an aspect ratio of approximately 4:1 and an elongated prismatic habit with subtly rounded terminations. Internally, it preserves well-developed concentric growth zoning that parallels the external morphology and encloses a xenomorphic relict core distinguished by strongly contrasting birefringence

(**Figure 5**, Grain 3). In longitudinal section parallel to the c-axis, the symmetry of the prismatic face {100} is clearly expressed. Under polarized light, discrete internal domains attain extinction at slightly different rotation angles, and abrupt transitions in interference colors across concentric growth zones are accompanied by local variations in extinction orientation. Deformation is expressed within the growth zoning as sharp shifts in interference colors between adjacent zones and as disruptions in zoning continuity. The zones are locally distorted, curved, or laterally offset rather than forming continuous concentric bands (**Figure 5**, Grain 3A, C). The relic core exhibits strongly contrasting interference colors and mosaic extinction (**Figure 5**, Grain 3B), and is composed of discrete optical domains that attain extinction at slightly different stage positions. This internal heterogeneity contrasts markedly with the comparatively uniform optical character of the surrounding overgrowth domains. Extremely thin, dark, planar lamellae occur as parallel to subparallel sets that attain complete extinction at specific stage orientations. These lamellae define regularly spaced arrays and intersect adjacent sets at variable angles.

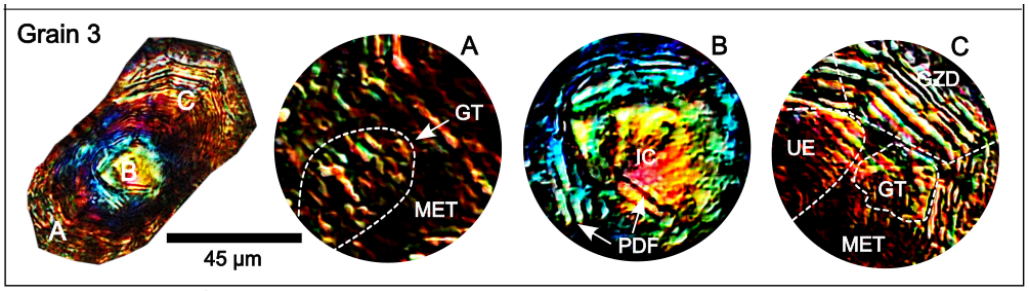

Figure 5. Representative euhedral crystal zircon containing metamorphic relict core (Grain 3) imaged under cross-polarized light, illustrating a range of internal microstructural features related to shock deformation.

Note: Left panels show full-grain views, whereas circular panels (A–C) present higher-magnification images of selected domains. The zircons record complex deformation patterns, including PDFs, granular textures (GT), disturbed growth zoning (GZD), inherited cores (IC), crystallographic misorientation (CM), metamict domains (MET), and undulatory extinction (UE). The spatial distribution and overprinting relationships among these features indicate heterogeneous shock strain accommodation at the grain scale.

5.4. Grain 4

The zircon crystal is visibly fractured and exhibits an elongated subhedral habit with sharply defined edges and an aspect ratio of approximately 4:1 (**Figure 6**, Grain 4). Concentric growth zoning, although locally discontinuous, broadly parallels the external crystal morphology. The heterogeneous birefringence and rectangular outline are consistent with a lateral, slightly oblique view of the prismatic face {100}. Rounded internal domains developed preferentially along the grain margins display diffuse boundaries, gradual variations in interference colors, and undulatory extinction. Planar deformation features occur as thin, closely spaced, parallel to subparallel lamellae (**Figure 6**, Grain 4A, C). Adjacent domains attain extinction at slightly different stage orientations, producing mosaic extinction (**Figure 6**, Grain 4B, C).

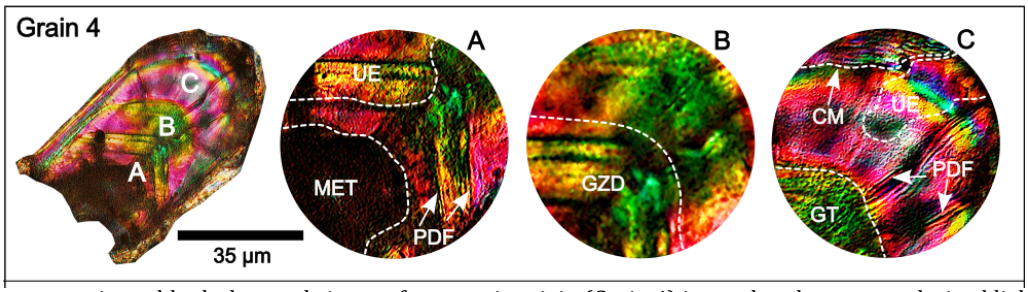

Figure 6. Representative subhedral crystal zircon of magmatic origin (Grain 4) imaged under cross-polarized light, displaying complex internal microstructures associated with shock-related deformation.

Note: Left panels show full-grain views, whereas circular panels (A–C) present higher-magnification images of selected domains. Abbreviations as in **Figures 3–5**.

5.5. Grain 5

The zircon crystal exhibits a short prismatic habit with locally well-defined edges, while other faces display slightly rounded contours. The dominant crystallographic form corresponds to the prismatic face {110}, with the c-axis oriented parallel to the image face (**Figure 7**, Grain 5). At the base of the crystal, domains with diffuse internal boundaries are characterized by gradual variations in birefringence. Adjacent sectors, by contrast, exhibit abrupt changes in interference colors, transitions from finely crystalline to granular textures, and mosaic extinction developed within discrete zones (**Figure 7**, Grain 5A). Along the lateral margins, concentric growth zoning is strongly distorted, exhibiting pronounced curvature and systematic deviations from the primary concentric geometry (**Figure 7**, Grain 5B, C). Planar fractures occur with variable orientations throughout both the basal and marginal regions.

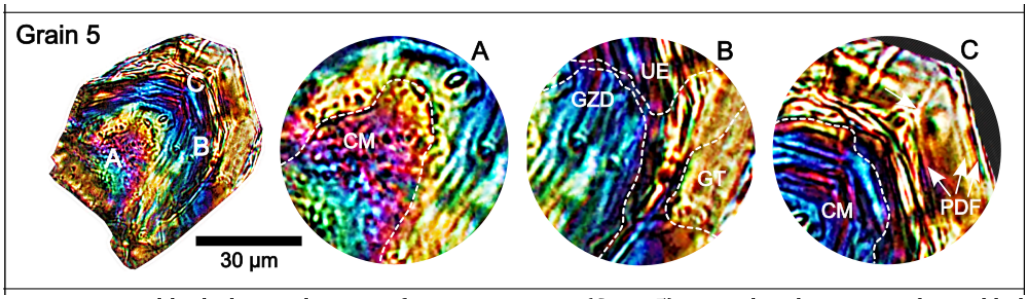

Figure 7. Representative subhedral crystal zircon of magmatic origin (Grain 5) imaged under cross-polarized light, displaying complex internal microstructures associated with shock-related deformation.

Note: Left panels show full-grain views, whereas circular panels (A–C) present higher-magnification images of selected domains. Abbreviations as in **Figures 3–5**.

5.6. Grain 6

The crystal exhibits an aspect ratio of approximately 4:1 and a slightly rhombohedral pyramidal termination associated with the prismatic form {110} (**Figure 8**, Grain 6). The crystallographic c-axis is oriented approximately parallel to the longest dimension of the crystal. Several sectors display undulatory extinction accompanied by locally reduced birefringence. Domains lacking discernible internal zoning occur as optically homogeneous or weakly birefringent patches that obscure primary growth structures; along the grain margins, diffuse and poorly defined zones are locally developed. Mosaic extinction is confined to discrete regions, where adjacent subdomains attain extinction at slightly different stage orientations (**Figure 8**, Grain 6A). Growth zoning is strongly disrupted, appearing segmented, discontinuous, and locally curved (**Figure 8**, Grain 6B). Thin, regularly spaced, dark lamellae occur as parallel to subparallel sets oriented obliquely relative to the growth zoning (**Figure 8**, Grain 6C).

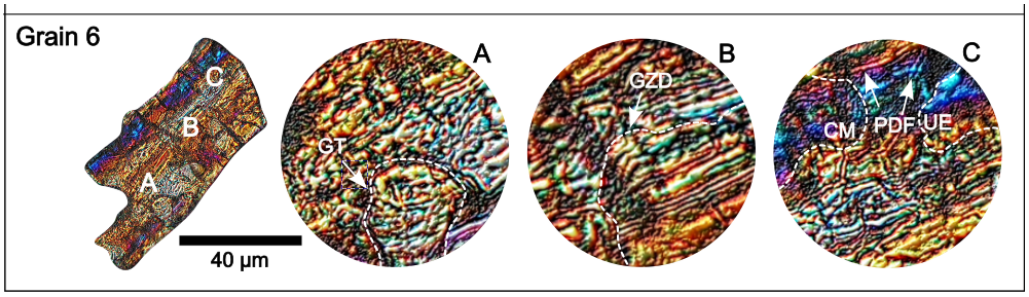

Figure 8. Representative subhedral crystal zircon of magmatic origin (Grain 6) imaged under cross-polarized light, displaying complex internal microstructures associated with shock-related deformation.

Note: Left panels show full-grain views, whereas circular panels (A–C) present higher-magnification images of selected domains. Abbreviations as in **Figures 3–5**.

6. Zircon Microdeformation as Indicators of Shock Metamorphism

Zircon remains highly resistant to recrystallization and chemical alteration even under extreme geological conditions. This resilience promotes the preservation of microstructural features in terranes subjected to intense weathering and tectonic overprinting [39,40]. Consequently, zircon constitutes a key mineral for identifying extensively modified impact craters, particularly where diagnostic macroscopic features—such as shatter cones and radial ejecta patterns—have been eroded or obliterated. In such settings, systematic microstructural analysis of zircon—especially targeting shock-related indicators such as partial recrystallization, PDFs, granular textures, and other microscale deformation structures—provides an independent, high-resolution line of evidence for confirming an impact origin [40,41].

Numerous studies have documented the diagnostic value of preserved shock microstructures in zircon and demonstrated their capacity to record hypervelocity impact signatures [17,40–44]. Owing to these properties, zircon-based approaches are particularly effective for investigating highly eroded or tectonically reworked impact structures in which subsequent geological processes have removed conventional macroscopic indicators.

Six representative zircon grains—subdivided into two morphological groups (euhedral metamorphic zircon: Grains 1–3; subhedral magmatic zircon: Grains 4–6)—were subjected to detailed microstructural analysis (**Figure 9**). Five primary deformation categories were identified: recrystallization, crystallographic misorientation, growth zoning disruption, planar deformation features (PDFs), and granular textures. Each feature was quantified by relative abundance (%) and ranked according to deformation intensity. The co-occurrence of multiple microstructural features within individual grains indicates a complex, polyphase deformation history [2,4,6].

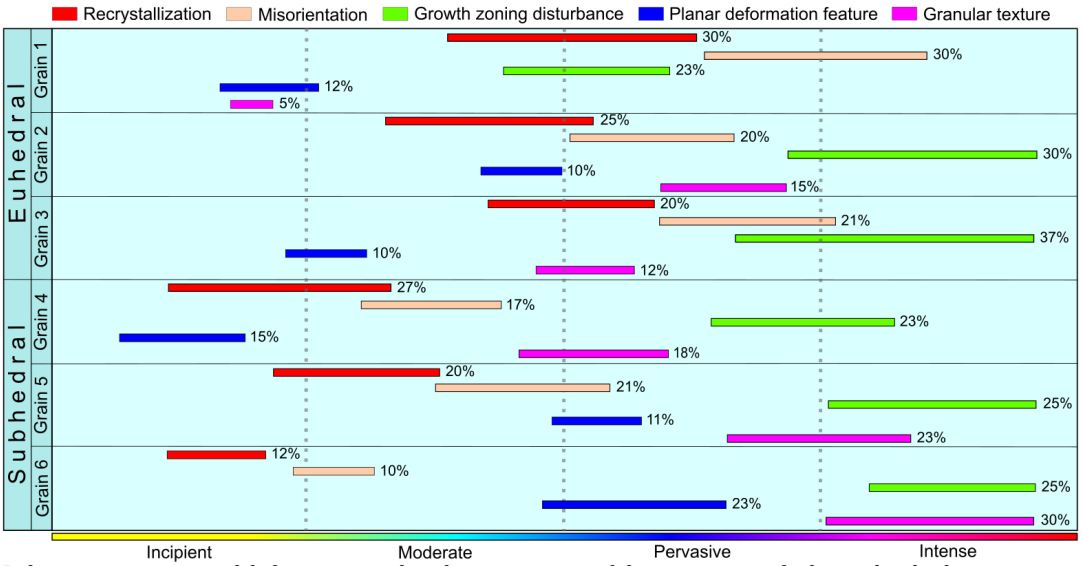

Figure 9. Relative proportions of deformation-related microstructural features quantified in individual zircon grains from the studied samples.

Note: The distribution of features highlights systematic variations in deformation style and intensity as a function of both shock level and grain morphology.

In the euhedral grains, recrystallization and crystallographic misorientation are the dominant deformation features, each reaching up to 30%, particularly in Grain 1. These features indicate that, despite the preservation of external crystal morphology, the grains experienced substantial thermal and mechanical overprinting following crystallization. Grain 2 exhibits 25% recrystallization and 30% growth zoning disruption, consistent with a significant thermal overprint. Grain 3, by contrast, displays the highest degree of internal deformation (37%), accompanied by 21% crystallographic misorientation and 20% recrystallization. Collectively, these observations support the interpretation of multiple superimposed thermo-mechanical events [8,13,15].

The subhedral grains display comparable deformation complexity, with more pronounced recrystallization and granular textures. Grain 4 exhibits 27% recrystallization, 23% growth zoning disruption, 17% crystallographic misorientation, and 15% PDFs, indicating exposure to high-pressure conditions. Grain 5 shows a more evenly distributed deformation pattern, comprising 20% recrystallization, 21% crystallographic misorientation, 25% growth zoning disruption, and 23% granular texture, indicative of pervasive polyphase deformation. The most intense overall deformation occurs in Grain 6, which records 23% PDFs, 30% granular texture, and 25% growth zoning disruption—features consistent with abrupt, high-strain events typically associated with shock-wave propagation [2,4].

The occurrence of PDFs in nearly all examined grains (10–23%) constitutes strong evidence for shock metamorphic processes. These microstructures are widely recognized as diagnostic indicators of high-pressure shock events associated with meteorite impacts [12,45,46]. Their co-occurrence with recrystallization textures and disrupted growth zoning further indicates overprinting by multiple deformation regimes, likely reflecting alternating high-pressure and high-temperature conditions. Growth zoning disruption, particularly in euhedral grains, records thermal and mechanical modification following crystallization. The higher proportions of recrystallization and granular textures in subhedral grains are consistent with dynamic recrystallization under intermediate- to high-temperature conditions [7,10].

The preferential localization of microdeformation along the prismatic crystal faces {100} and {110} provides important constraints on the deformation history of the analysed zircon grains. These faces correspond to directions within the tetragonal zircon lattice characterized by lower atomic bond density and greater interatomic spacing relative to basal faces such as {001} [4,8,13,15]. Consequently, they represent mechanically weaker, energetically favorable sites for stress accommodation [46,47] and exhibit lower critical resolved shear stresses. These conditions promote dislocation nucleation and glide, intracrystalline misorientation, and PDF formation [48,49]. Such crystallographic anisotropy exerts a primary control on zircon deformation, with slip preferentially occurring along prismatic faces and producing localized strain accumulation [50]. The concentration of deformation along these mechanically susceptible faces indicates a directionally constrained, anisotropic stress field, consistent with rapid, high-strain events associated with shock-wave propagation during meteorite impact—wherein deformation localizes along crystallographically favored slip systems rather than being uniformly distributed throughout the crystal lattice [10,13,15].

The face {100}, oriented parallel to the c-axis, preferentially accommodates vertical compressive stresses or lateral shear, whereas the face {110} records oblique and complex strain patterns characteristic of high-pressure, high-temperature environments. Preferential activation of these crystallographic directions, therefore, reflects the original grain orientations at the time of deformation and constrains the geometry and magnitude of the imposed stress fields. Furthermore, PDFs developing obliquely to these faces constitute unequivocal evidence of high-energy shock deformation [40,45], recording selective reorganization of the crystal lattice under extreme stress conditions [47].

Partial recrystallization and granular textures are likewise concentrated along these faces, supporting a mechanism of internal energy dissipation under dynamic deformation. This observation reinforces the interpretation that the analyzed zircon grains record multiple deformation episodes, characterized by progressive recrystallization and stress redistribution along structurally susceptible crystallographic orientations [2,4,14].

A critical reassessment of two alternative hypotheses—regional tectonic deformation and re-metamorphism—demonstrates that neither satisfactorily accounts for the full spectrum of observed microstructures. An impact origin remains the only interpretation consistent with the complete dataset. The tectonic hypothesis is rejected primarily on the basis of the absence of regional structures capable of generating localized, high-strain-rate deformation in mechanically resilient minerals such as zircon [21,28]. Moreover, the spatial distribution of shock microstructures—including deformation lamellae and recrystallization bands—is

highly restricted and heterogeneous, in sharp contrast to the pervasive and systematic patterns characteristic of tectono-metamorphic deformation [4,7,12].

Re-metamorphism is similarly inconsistent with the mineralogical and textural constraints. The host lithological unit lacks metamorphic associations indicative of the temperatures or pressures required to produce the documented microstructures [28]; notably, neoblastic growth of index minerals (e.g., garnet, staurolite, sillimanite) is absent, and no evidence for diffuse, large-scale recrystallization has been identified [21]. Although certain zircon microstructures may develop under high-grade metamorphic conditions, such processes require extreme pressure–temperature regimes [8] unsupported by either the stratigraphic record or mineralogical re-equilibration [21,28]. Furthermore, the observed microstructures exhibit diagnostic signatures of ultra-rapid, high-pressure deformation—including multidirectional microfractures and crystallographically controlled lamellae—that are incompatible with the prolonged, low-strain-rate conditions characteristic of progressive or static metamorphism [4,13,18].

Multiple independent lines of evidence converge on an impact event as the most plausible mechanism [20,30,31]. The most compelling evidence is the direct spatial correlation between zircon microstructures and other mineralogical shock signatures, reinforcing their interpretation as features diagnostic of impact processes [33]. Quartz from the relevant stratigraphic intervals contains well-preserved PDFs [30], arranged in multiple parallel sets with characteristic crystallographic orientations, whose formation requires transient pressure pulses far exceeding those generated by tectonic compression.

Further support derives from the occurrence of Fe–Mg–Si-rich spherules at the same stratigraphic level, interpreted as condensates from an impact-generated plume [32]. Their morphology, chemical composition, and sedimentary context are consistent with well-documented impact-related systems and have no plausible volcanic, tectonic, or metamorphic counterparts [32].

Microdeformation analysis of zircon from the Colônia impact crater constrains both the intensity and the nature of the tectonothermal processes experienced by this mineral. Systematic mapping of deformation along the crystallographic faces {100} and {110} permits reconstruction of strain patterns while simultaneously providing thermodynamic constraints for modelling post-impact processes and regional geological evolution. Integration of intracrystalline deformation data reveals complex overprinting histories, underscoring the sensitivity of zircon to subtle but geologically significant local thermodynamic variations. Furthermore, the anisotropic distribution of microdeformation constitutes a robust diagnostic criterion for distinguishing shock metamorphism from regional metamorphism and magmatic overprinting.

7. Conclusions

Detailed examination of six representative grains from a population of 40 zircon crystals provides critical insights into the mineral's deformation behavior during shock metamorphism. Microstructural analysis reveals diagnostic features of dynamic recrystallization and stress accommodation under high-pressure–high-temperature conditions. These results refine current understanding of micromechanical processes during impact cratering and underscore the significance of zircon as a mechanically robust, chemically stable mineral under extreme geological conditions. The principal evidence for the mechanical response of zircon under such conditions is summarized as follows:

The systematic occurrence of PDFs, crystallographic misorientation, disrupted growth zoning, and granular textures across a wide range of grain morphologies reflects a complex, polyphase deformation history characteristic of hypervelocity impact events.

The occurrence of PDFs—particularly when associated with other deformation textures—unequivocally indicates shock pressures exceeding those attainable during endogenous metamorphism, thereby confirming the impact origin of the analyzed samples.

Crystallographic orientation exerts a strong control on deformation behavior, with stress preferentially accommodated along the prismatic faces {100} and {110}.

Microstructural preservation differences between euhedral and subhedral grains indicate heterogeneous

post-impact thermal and mechanical overprinting, consistent with differential recrystallization pathways under variable pressure–temperature conditions.

Intracrystalline deformation mapping in zircon constitutes a high-resolution tool for constraining both the intensity and temporal evolution of impact-related processes, enhancing the recognition and interpretation of eroded or tectonically overprinted impact structures.

The preservation of shock-related microdeformation features in zircon—even within weathered and reworked terranes—confirms its reliability as a robust mineralogical proxy for identifying impact events.

The concurrence of high-pressure zircon microtextures, shock-diagnostic planar deformation features in quartz [20], and spherule-bearing deposits [32] constitutes a robust, internally consistent evidential framework that effectively excludes regional tectonic deformation and subsequent metamorphism as viable alternative explanations. The integrated dataset strongly supports an impact origin for the microstructural features preserved in the studied zircon grains.

Author Contributions

All authors contributed to data integration, interpretation, and manuscript preparation equally. All authors have read and agreed to the published version of the manuscript.

Funding

Financial support for this study (Fieldwork for sample collection and preparation of thin sections) was provided by the São Paulo Research Foundation (FAPESP) through grants 2011/50987-0 and 2012/50042-9.

Institutional Review Board Statement

Not applicable.

Informed Consent Statement

Not applicable.

Data Availability Statement

All analytical data are included in the main text.

Acknowledgments

Several colleagues generously contributed comments and feedback during the preparation of this manuscript. We thank our colleagues from EACH-USP and IG-IPA for their invaluable support. We also acknowledge SABESP for providing the samples. W. Sallun Filho acknowledges CNPq for the research grant. We appreciate the anonymous reviewers for their constructive comments, which significantly improved the quality of the manuscript.

Conflicts of Interest

The authors declare no conflict of interest.

References

[1] Pidgeon, R.T., Nemchin, A.A., Kamo, S.L., 2011. Comparison of structures in zircons from lunar and terrestrial impactites. Canadian Journal of Earth Sciences. 48(2), 107–116. DOI: https://doi.org/10.1139/E10-037

[2] Rubatto, D., 2017. Zircon: The Metamorphic Mineral. Reviews in Mineralogy and Geochemistry. 83(1), 261–295. DOI: https://doi.org/10.2138/rmg.2017.83.9

[3] Costa, F., 2021. Clocks in Magmatic Rocks. Annual Review of Earth and Planetary Sciences. 49(1), 231–252. DOI: https://doi.org/10.1146/annurev-earth-080320-060708

[4] Osinski, G.R., Grieve, R.A.F., Ferrière, L., et al., 2022. Impact Earth: A review of the terrestrial impact record. Earth-Science Reviews. 232, 104112. DOI: https://doi.org/10.1016/j.earscirev.2022.104112

[5] Chinchalkar, N.S., Osinski, G.R., Erickson, T.M., et al., 2024. Zircon microstructures record high temperature and pressure conditions during impact melt evolution at the West Clearwater Lake impact structure, Canada. Earth and Planetary Science Letters. 636, 118714. DOI: https://doi.org/10.1016/j.epsl.2024.118714

[6] Cavosie, A.J., Timms, N.E., Erickson, T.M., et al., 2016. Transformations to granular zircon revealed: Twinning, reidite, and ZrO2 in shocked zircon from Meteor Crater (Arizona, USA). Geology. 44(9), 703–706. DOI: https://doi.org/10.1130/G38043.1

[7] Timms, N.E., Erickson, T.M., Pearce, M.A., et al., 2017. A pressure-temperature phase diagram for zircon at extreme conditions. Earth-Science Reviews. 165, 185–202. DOI: https://doi.org/10.1016/j.earscirev.2016.12.008

[8] Nan, S., Wang, S., Zhang, F., et al., 2024. Zircon-to-reidite phase transition enhanced by minor radiation damage: Implications for hypervelocity impacts. Chemical Geology. 654, 122041. DOI: https://doi.org/10.1016/j.chemgeo.2024.122041

[9] Timms, N.E., Healy, D., Erickson, T.M., et al., 2018. Role of Elastic Anisotropy in the Development of Deformation Microstructures in Zircon. In: Moser, D.E., Corfu, F., Darling, J.R., et al. (Eds.). Geophysical Monograph Series. Wiley: London, UK. pp. 183–202. DOI: https://doi.org/10.1002/9781119227250.ch8

[10] Cavosie, A.J., Timms, N.E., Ferrière, L., et al., 2018. FRIGN zircon—The only terrestrial mineral diagnostic of high-pressure and high-temperature shock deformation. Geology. 46(10), 891–894. DOI: https://doi.org/10.1130/G45079.1

[11] Erickson, T.M., Pearce, M.A., Reddy, S.M., et al., 2017. Microstructural constraints on the mechanisms of the transformation to reidite in naturally shocked zircon. Contributions to Mineralogy and Petrology. 172(1), 6. DOI: https://doi.org/10.1007/s00410-016-1322-0

[12] Zhao, J., Xiao, L., Xiao, Z., et al., 2021. Shock-deformed zircon from the Chicxulub impact crater and implications for cratering process. Geology. 49. DOI: https://doi.org/10.1130/G48278.1

[13] Ross, C.H., Stockli, D.F., Erickson, T., et al., 2024. Zircon (U-Th)/He impact crater thermochronometry and the effects of shock microstructures on He diffusion kinetics. Geochimica et Cosmochimica Acta. 373, 308–325. DOI: https://doi.org/10.1016/j.gca.2023.12.028

[14] Wittmann, A., Kenkmann, T., Schmitt, R.T., et al., 2006. Shock-metamorphosed zircon in terrestrial impact craters. Meteoritics & Planetary Science. 41(3), 433–454. DOI: https://doi.org/10.1111/j.1945-5100.2006.tb00472.x

[15] Tartèse, R., Endley, S., Joy, K.H., 2022. U-Pb dating of zircon and monazite from the uplifted Variscan crystalline basement of the Ries impact crater. Meteoritics & Planetary Science. 57(4), 830–849. DOI: https://doi.org/10.1111/maps.13798

[16] Zhao, J., Xiao, L., Xiao, Z., et al., 2025. Element Redistribution and Age Resetting in Shock-Deformed Zircon from the Chicxulub Impact Structure. Geochimica et Cosmochimica Acta. 393, 219–237. DOI: https://doi.org/10.1016/j.gca.2025.01.021

[17] Erickson, T.M., Timms, N.E., Kirkland, C.L., et al., 2017. Shocked monazite chronometry: Integrating microstructural and in situ isotopic age data for determining precise impact ages. Contributions to Mineralogy and Petrology. 172(2–3), 11. DOI: https://doi.org/10.1007/s00410-017-1328-2

[18] Schwarz, W.H., Hanel, M., Trieloff, M., 2020. U-Pb dating of zircons from an impact melt of the Nördlinger Ries crater. Meteoritics & Planetary Science. 55(2), 312–325. DOI: https://doi.org/10.1111/maps.13437

[19] Velázquez, V.F., Riccomini, C., Sobrinho, J.M.A., et al., 2013. Evidence of Shock Metamorphism Effects in Allochthonous Breccia Deposits from the Colônia Crater, São Paulo, Brazil. International Journal of Geosciences. 4(1), 274–282. DOI: https://doi.org/10.4236/ijg.2013.41A025

[20] Kollert, R., Björnberg, A., Davino, A., 1961. Preliminary studies of a circular depression in the Colônia region, Santo Amaro, São Paulo. Boletim da Sociedade Brasileira de Geologia. 3, 57–77. (in Portuguese)

[21] Coutinho, J.M.V., 1980. Geological Map of Greater São Paulo, 1:100,000. Emplasa: São Paulo, Brazil. (in Portuguese)

[22] Motta, U.S., Flexor, J.M., 1991. Gravimetric Study of the Circular Depression of Colônia, São Paulo, Brazil. In Proceedings of the 2nd International Congress of the Brazilian Geophysical Society, Bahia, Brazil, 27 October–1 November 1991. DOI: https://doi.org/10.3997/2214-4609-pdb.316.28 (in Portuguese)

[23] Masero, W.C.B., Fontes, S.L., 1992. Geoelectrical studies of the Colônia impact structure, Santo Amaro, State of São Paulo—Brazil. Revista Brasileira de Geofísica. 10(5), 25–41.

[24] Neves, F.A., 1998. Study of the circular depression of Colônia, São Paulo (SP), using the seismic method. Revista Brasileira de Geociências. 28, 3–10. (in Portuguese)

[25] Riccomini, C., Turcq, B.J., Martin, L. 1989. The Colônia astrobleme. In Proceedings of the International Symposium on Global Changes in South America during the Quaternary: Past, Present and Future, São Paulo, Brazil, 8–12 May 1989.

[26] Riccomini, C., Turcq, B.J., Moreira, M.Z., et al., 1991. The Colônia astrobleme, Brazil. Revista do Instituto Geológico. 12, 87–94.

[27] Riccomini, C., Neves, F.A., Turcq, B.J., 1992. Colônia astrobleme (São Paulo, Brazil): Current state of knowledge. In Proceedings of the 37th Brazilian Congress of Geology, São Paulo, Brazil, 9–15 December 1992. (in Portuguese)

[28] Riccomini, C., Turcq, B.J., Ledru, M.P., et al., 2005. Colônia Crater, São Paulo: A probable astrobleme with Quaternary paleoclimate records in the Greater São Paulo region. In: Winge, M., Schobben-

haus, C., Berbert-Born, M., et al. (Eds.). Geological and Paleontological Sites of Brazil. Serviço Geológico do Brasil (CPRM): Brasília, Brazil. pp. 35–44. (in Portuguese)

[29] Riccomini, C., Crósta, A.P., Prado, R.L., et al., 2011. The Colônia structure, São Paulo, Brazil. Meteoritics & Planetary Science. 46(11), 1630–1639. DOI: https://doi.org/10.1111/j.1945-5100.2011.01252.x

[30] Velázquez, V.F., Lucena, R.F., Sobrinho, J.M.A., et al., 2017. Petrographic Investigation of Target Rock Transformation under High Shock Pressures from the Colônia Impact Crater, Brazil. Earth Science Research. 7(1), 13. DOI: https://doi.org/10.5539/esr.v7n1p13

[31] Velázquez, V.F., Gomes, C.B., Mansueto, M., et al., 2021. Morphological aspects, textural features and chemical composition of spherules from the Colônia impact crater, São Paulo, Brazil. Solid Earth Sciences. 6(1), 27–36. DOI: https://doi.org/10.1016/j.sesci.2020.12.004

[32] Velazquez, V.F., Sobrinho, J.M.A., Lucena, R.F., et al., 2024. Mechanical Microdeformation and Kink–band Formation in Mica from the Colônia Impact Crater, São Paulo, Brazil. Earth Science Research. 13(1), 1. DOI: https://doi.org/10.5539/esr.v13n1p1

[33] Klein, C., Dutrow, B., 2007. Manual of Mineral Science, 23rd ed. Wiley: Hoboken, NJ, USA.

[34] Nesse, W.D., Baird, G.B., 2023. Introduction to Mineralogy, 4th ed. Oxford University Press: Oxford, UK.

[35] Deer, W.A., Howie, R.A., Zussman, J., 2013. An Introduction to the Rock-Forming Minerals, 3rd ed. Mineralogical Society of Great Britain and Ireland: Middlesex, UK.

[36] Dias, B.M., Velázquez, V.F., Lucena, R.F., et al., 2020. Petrographic Microscope Digital Image Processing Technique for Texture and Microstructure Interpretation of Earth Materials. Earth Science Research. 9(1), 58. DOI: https://doi.org/10.5539/esr.v9n1p58

[37] Hoskin, P.W.O., Black, L.P., 2000. Metamorphic zircon formation by solid-state recrystallization of protolith igneous zircon. Journal of Metamorphic Geology. 18(4), 423–439. DOI: https://doi.org/10.1046/j.1525-1314.2000.00266.x

[38] Bohor, B.F., Betterton, W.J., Krogh, T.E., 1993. Impact-shocked zircons: Discovery of shock-induced textures reflecting increasing degrees of shock metamorphism. Earth and Planetary Science Letters. 119(3), 419–424. DOI: https://doi.org/10.1016/0012-821X(93)90149-4

[39] Guerrero, D., Reimold, W.U., Hauser, N., et al., 2025. Shock deformation and U-Pb isotope systematics in zircon from impactites of the Rochechouart impact structure: Impact age and zircon provenance. Geochimica et Cosmochimica Acta. 402, 338–358. DOI: https://doi.org/10.1016/j.gca.2025.05.049

[40] Martell, J., Alwmark, C., Holm-Alwmark, S., et al., 2021. Shock deformation in zircon grains from the Mien impact structure, Sweden. Meteoritics & Planetary Science. 56(2), 362–378. DOI: https://doi.org/10.1111/maps.13625

[41] Garde, A.A., Johansson, L., Keulen, N., et al., 2023. Zircon Microstructures in Large, Deeply Eroded Impact Structures and Terrestrial Seismites. Journal of Petrology. 64(11), egad079. DOI: https://doi.org/10.1093/petrology/egad079

[42] Krogh, T.E., Kamo, S.L., Bohor, B.F., 2013. Shock Metamorphosed Zircons With Correlated U-Pb Discordance and Melt Rocks With Concordant Protolith Ages Indicate an Impact Origin for the Sudbury Structure. In: Basu, A., Hart, S. (Eds.). Geophysical Monograph Series. American Geophysical Union: Washington, DC, USA. pp. 343–353. DOI: https://doi.org/10.1029/GM095p0343

[43] Plan, A., Kenny, G.G., Erickson, T.M., et al., 2021. Exceptional preservation of reidite in the Rochechouart impact structure, France: New insights into shock deformation and phase transition of zircon. Meteoritics & Planetary Science. 56(10), 1795–1828. DOI: https://doi.org/10.1111/maps.13723

[44] Erickson, T.M., Cavosie, A.J., Moser, D.E., et al., 2013. Correlating planar microstructures in shocked zircon from the Vredefort Dome at multiple scales: Crystallographic modeling, external and internal imaging, and EBSD structural analysis. American Mineralogist. 98(1), 53–65. DOI: https://doi.org/10.2138/am.2013.4165

[45] Zhang, N., Asle Zaeem, M., 2019. Effects of Crystal Orientation and Pre-existing Defects on Nanoscale Mechanical Properties of Yttria-Stabilized Tetragonal Zirconia Thin Films. JOM. 71(11), 3869–3875. DOI: https://doi.org/10.1007/s11837-019-03725-z

[46] Reddy, S.M., van Riessen, A., Saxey, D.W., et al., 2016. Mechanisms of deformation-induced trace element migration in zircon resolved by atom probe and correlative microscopy. Geochimica et Cosmochimica Acta. 195, 158–170. DOI: https://doi.org/10.1016/j.gca.2016.09.019

[47] Glazovskaya, L.I., Shcherbakov, V.D., Piryazev, A.A., 2024. Logoisk impact structure, Belarus: Shock transformation of zircon. Meteoritics & Planetary Science. 59(1), 88–104. DOI: https://doi.org/10.1111/maps.14110

[48] Kovaleva, E., Klötzli, U., Habler, G., et al., 2014. Finite lattice distortion patterns in plastically de-

formed zircon grains. Solid Earth. 5(2), 1099–1122. DOI: https://doi.org/10.5194/se-5-1099-2014

[49] Timms, N.E., Reddy, S.M., Healy, D., et al., 2012. Resolution of impact-related microstructures in lunar zircon: A shock-deformation mechanism map. Meteoritics & Planetary Science. 47(1), 120–141. DOI: https://doi.org/10.1111/j.1945-5100.2011.013 16.x

[50] Kovaleva, E., Klötzli, U., Wheeler, J., et al., 2018. Mechanisms of strain accommodation in plastically-deformed zircon under simple shear deformation conditions during amphibolite-facies metamorphism. Journal of Structural Geology. 107, 12–24. DOI: https://doi.org/10.1016/j.jsg.2017.11.015